JOC The Journal of Organic Chemistry

Article

pubs.acs.org/joc

Theoretical Insights into the Catalytic Mechanism of *N*-Heterocyclic Olefins in Carboxylative Cyclization of Propargyl Alcohol with CO_2

Weiyi Li,*[,†] Na Yang,[‡] and Yajing Lyu[†]

[†]School of Science, Xihua University, Chengdu, Sichuan 610039, P. R. China

[‡]Institute of Nuclear Physics and Chemistry, China Academy of Engineering Physics, Mianyang 621900, P. R. China

Supporting Information

ABSTRACT: The mechanism of carboxylative cyclization of propargyl alcohol with CO_2 catalyzed by *N*-heterocyclic olefins (NHOs) has been studied by density functional theory calculations. The calculations reveal that the catalytic reaction tends to proceed via the NHO-mediated basic ionic pair mechanism, in which free NHO primarily acts as a basic precursor to trigger the carboxylation of propargyl alcohol with CO_2, leading to a $[NHOH]^+[carbonate]^-$ ion pair intermediate. Then, the catalytic cycle proceeds, including isomerization of the $[NHOH]^+[carbonate]^-$ ion pair intermediate, intramolecular nucleophilic addition of the carbonate oxygen anion to the alkynyl group, and protonation of the alkenyl carbon anion with an external propargyl alcohol molecule. Molecule orbital and nature population analysis discloses that the preference for the basic ionic pair mechanism is due to the favorable orbital and charge interactions between the α-carbon atom of NHO and the hydroxyl hydrogen of propargyl alcohol. The $[NHOH]^+$ cation has proven to be crucial for stabilizing the $[carbonate]^-$ anion, which allows the reaction to proceed through a more thermodynamically stable pathway. The investigations of the effect of substituents of NHOs predict that *N*-substituents with a strong electron donating effect and a bulky steric effect might improve the catalytic activity of NHOs for the reaction.

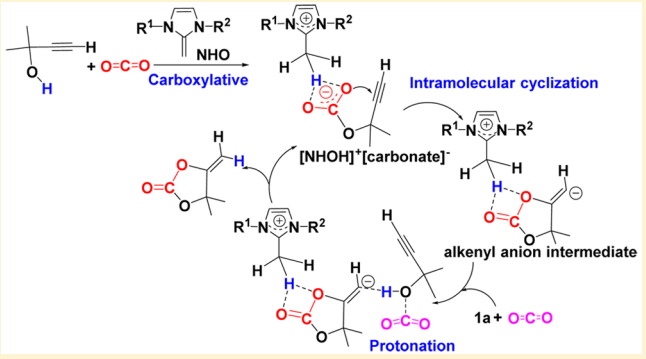

1. INTRODUCTION

Today, the catalytic transformation of carbon dioxide (CO_2) is of increasing interest for producing highly value-added chemicals, such as methane,[1] methanol,[2] formic acid,[3] cyclic carbonates,[4] etc., because CO_2 is regarded as both a greenhouse gas that causes global warming problems and a highly abundant, inexpensive, nontoxic, nonflammable, and renewable C1 resource.[5] However, the thermodynamic stability of CO_2 is still one of the roadblocks on the way to its utilization. Consequently, the development of more powerful and efficient catalysts for the activation of CO_2 is of great importance and a long-standing goal of chemists.

Very recently, the alkylidene derivatives of the well-known *N*-heterocyclic carbenes (NHCs), termed *N*-heterocyclic olefins (NHOs), have emerged as a new class of valuable organocatalysts.[6] Because of the aromatization of the *N*-heterocyclic ring in *N*,*N*′-disubstituted 2-methylene imidazolines, the nucleophilicity and basicity of the α-carbon atoms in NHOs are often stronger than those of the carbene centers in NHCs.[7] Thus, NHOs and their derivatives have been established as a prevalent family of end-on ligands in transition metal coordination[7,8] and organocatalysts in CO_2 fixation and polymerization reactions.[9] In 2013, Lu and co-workers reported the synthesis of a series of NHOs using 2-methyl imidazolium iodide as a starting material (Scheme 1, reaction 1).[9a] The

Scheme 1. Synthesis of NHO−CO_2 Adducts and Their Application in Catalyzing Carboxylative Cyclization of Propargylic Alcohols with CO_2

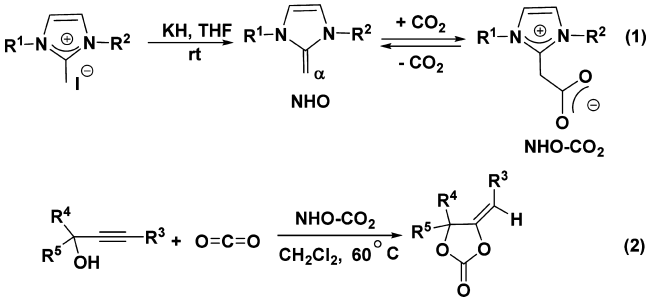

activation of NHO to CO_2 is proven by the formation of zwitterionic NHO−CO_2 adducts, in which the linear geometry of the O=C=O moiety in the ground state is changed to be bent with an O−C−O angle of 127.7−129.9°.[9a] The analogue bent geometries of the O=C=O moiety are observed in other CO_2-based metal complexes, such as nickel(0),[10a,b] cobalt(I),[10c] Rh(I),[10d] etc., NHC−CO_2 adducts,[11a−c] and guanidine−CO_2

Received: March 15, 2016
Published: June 6, 2016

DOI: 10.1021/acs.joc.6b00559
J. Org. Chem. 2016, 81, 5303−5313

Scheme 2. Plausible Catalytic Cycles for Carboxylative Cyclization of Propargyl Alcohols with CO_2 Catalyzed by NHOs

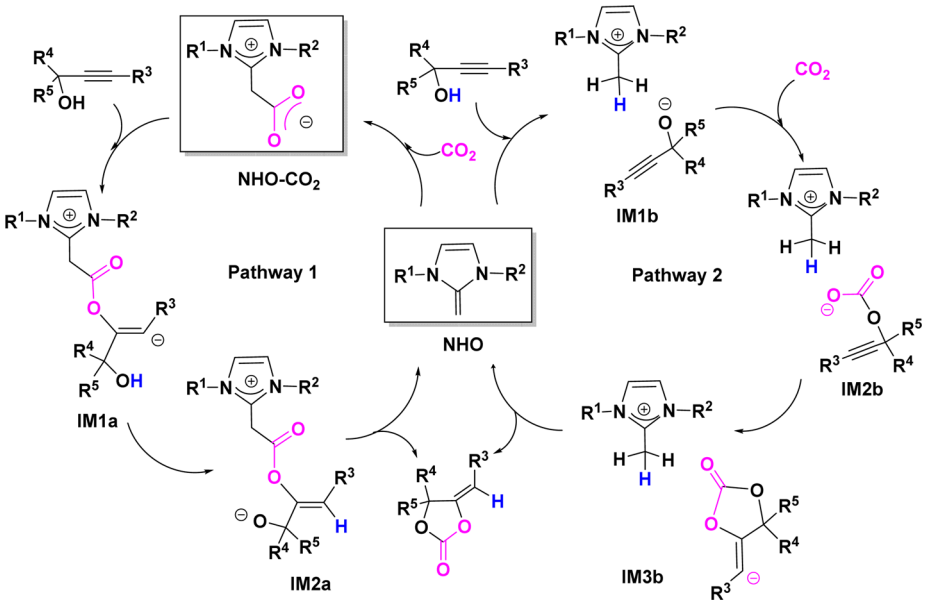

adducts.[11d] On the other hand, the resultant NHO−CO_2 adducts are also found to be very effective in promoting carboxylative cyclization of propargylic alcohols with CO_2 to give α-alkylidene cyclic carbonates (Scheme 1, reaction 2),[9a] which are versatile intermediates or precursors in organic synthesis and polymer chemistry.[12] With respect to the already existing metallic catalysts (e.g., Ru,[13a] Co,[13b] Cu,[13c,d] Pd,[13e] and Ag[13f,g] species) used for the reaction, organocatalysts, with the advantages of being more inexpensive and environmentally friendly, have attracted unprecedented attention over the past decade. Among the reported organocatalytic systems, including nBu$_3$P,[14] guanidines,[15] NHC−CO_2 adducts,[16] and P−ylide adducts,[17] NHO−CO_2 adducts also show a comparable or better catalytic effect in improving the yield of the product, accelerating the reaction rate, lowering the catalyst loading, and expanding the substrate scope of propargylic alcohols.

Although NHO−CO_2 adducts exhibit high catalytic potential in the carboxylative cyclization reaction, the actual active species and the detailed catalytic mechanisms are ambiguous. This is because the decomposition of NHO−CO_2 adducts to free NHOs and CO_2 is inevitable as the reaction temperature increases.[9a] Both NHO−CO_2 adducts and free NHOs have a certain catalytic activity and might promote the reaction. The analogue phenomena are observed in a number of NHC-catalyzed CO_2 transformations, of which catalytic mechanisms have been successfully elucidated by means of quantum chemistry calculations.[18] In terms of this fact, two possible mechanisms, differing in the catalytic role of free NHOs, were experimentally proposed for the carboxylative cyclization reaction examined here (Scheme 2).[9a] One is through a nucleophilic addition mechanism (pathway 1), in which a CO_2 molecule is initially activated by the nucleophilic NHOs with the formation of NHO−CO_2 adducts. Then, the carboxylate oxygen anion of NHO−CO_2 adducts attacks the C≡C bond of propargyl alcohols to give an alkenyl anion intermediate **IM1a**. Finally, the protonation of the alkenyl anion and intramolecular cyclization allow the production of α-alkylidene cyclic carbonates and the recovery of free NHOs. Alternatively, the catalytic reaction might proceed through a basic ionic pair mechanism (pathway 2), in which NHOs act primarily as a base to abstract the hydroxyl hydrogen atom of propargyl alcohols, leading to a $[NHOH]^+[alkoxide]^-$ ionic pair intermediate **IM1b**. The alkoxide anion with high nucleophilicity can easily capture one molecule of CO_2 to form a $[NHOH]^+[carbonate]^-$ ionic pair intermediate **IM2b**. From **IM2b**, the intramolecular nucleophilic addition from the carbonate anion to the C≡C bond and the pronation of the alkenyl anion with $[NHOH]^+$ cation lead to the formation of α-alkylidene cyclic carbonate and regeneration of free NHOs. To clarify the real role of free NHOs, some deuterium labeling isotope analysis was also conducted by Lu and co-workers.[9a] However, the limited experimental results are too insufficient to determine the actual reaction course and understand the catalytic role of NHOs.

Because of the great potential of NHOs in synthetic chemistry and a lack of investigation of their activation mechanisms, we performeda comprehensive theoretical study of NHO-catalyzed carboxylative cyclization of propargylic alcohols with CO_2. Through a detailed mechanistic studies, we hope to provide important insights into the understanding of the catalytic role of NHOs in carboxylative cyclization reactions, which may optimize and/or improve reaction conditions, characterization of NHOs catalytic systems, and extension of their application to a broader range of CO_2 transformations.

2. COMPUTATIONAL METHODS

To disclose the catalytic mechanism of NHOs in carboxylative cyclization of propargylic alcohols with CO_2, a density functional theory (DFT) calculation of such a reaction was performed with Gaussian 09.[19] All geometries of the reactants, products, intermediates (IM), and transition states (TS) involved in this mechanistic study were fully optimized in CH_2Cl_2 solvent (experimentally used) with the continuum solvation model (SMD[20]) at the M06-2X[21]/6-31+G*[22] level of theory. This method has already been examined to be efficient and reliable in our previous study of the structure−activity relationship of free NHOs and NHO−CO_2 adducts with various kinds of substituents at the N- and C-termini of the imidazolium ring.[23] The vibrational frequency calculations at the same level of theory were conducted to characterize each optimized structure is an intermediate (with no imaginary frequency) or a transition state (with one imaginary frequency) and obtain the thermal corrections at 298 K.

DOI: 10.1021/acs.joc.6b00559
J. Org. Chem. 2016, 81, 5303−5313

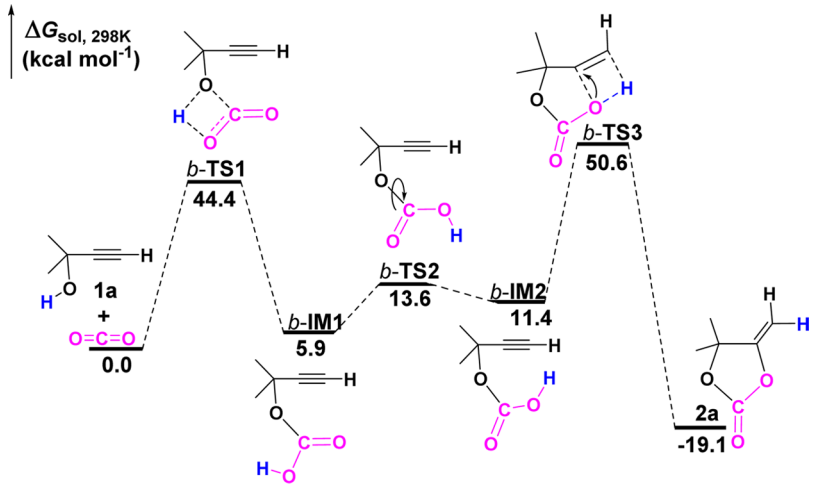

Figure 1. Energy profile for uncatalyzed carboxylative cyclization of **1a** with CO_2 calculated at the M06-2X(SMD, CH_2Cl_2)/6-311++G**//M06-2X(SMD, CH_2Cl_2)/6-31+G* level.

Intrinsic reaction coordinate (IRC[24]) scans were conducted when necessary to check that the transition state correctly connects the two relevant minima. To improve the accuracy of the energy, the single-point energy of each optimized structure was calculated at the M06-2X (SMD, CH_2Cl_2)/6-311++G** level. The relative free energy (ΔG_{sol}) was obtained by combining the single-point energy with Gibbs free energy correction at the M06-2X/6-31+G* level. In addition, an adjustment for the change in standard state from 1 atm to a concentration of 1 M of RT ln(24.5), 1.9 kcal mol^{-1}, was applied for all the species in solution. Because the present reaction involves component changes, the translation and rotational entropy loss in intermediates and transition states will be significantly overestimated if the separated reactants are used as the energy reference. On the basis of "the theory of free volume",[25a] a correction of 2.6 kcal mol^{-1} per component change for a reaction [i.e., a reaction from m to n components has an additional correction of $(n - m) \times 2.6$ kcal mol^{-1}] was made in the same manner used by many earlier theoretical studies.[25b−d] Unless otherwise specified, the relative free energy (ΔG_{sol}, 298 K, 1 M), including the thermal correction, standard state correction, and entropy correction, is discussed in the ext. The relative enthalpy (ΔH_{sol}) and relative free energy without entropy correction ($\Delta G_{sol,wec}$) are given in the Supporting Information for reference. In addition, natural bond orbital (NBO[26]) analysis of the key species was conducted to gain insight into the electronic properties of the system.

3. RESULTS AND DISCUSSION

3.1. Background Reaction without a Catalyst. Initially, the reaction pathway for carboxylative cyclization of propargyl alcohol **1a** with CO_2 in the absence of catalysts was explored as an ideal benchmark for discussing the catalytic reaction under free NHOs or NHO−CO_2 adducts. As shown in Figure 1, the uncatalyzed carboxylative cyclization reaction of **1a** with CO_2 is composed of three elementary steps. The first step is the carboxylation of **1a** with CO_2 through a concerted four-center *b*-**TS1** (44.4 kcal mol^{-1}), leading to *b*-**IM1**. Then, the hydroxyl group of the carbonate moiety orients toward the propargyl moiety in *b*-**IM2**, as a consequence of the C−O bond rotation over *b*-**TS2** (13.6 kcal mol^{-1}). With this conformation, *b*-**IM2** can be ready to undergo an intramolecular nucleophilic addition from the carboxyl oxygen atom to the C≡C bond, resulting in ring-closure product **2a**. This process via *b*-**TS3** (50.6 kcal mol^{-1}) contains the initial hydrogen transfer from the carboxyl group to the terminal carbon atom of the alkynyl group, followed by the nucleophilic attack of the carboxyl oxygen atom on the middle carbon atom of the alkynyl group. Although the formation of **2a** is exoergic by 19.1 kcal mol^{-1} in free energy, the carboxylative cyclization of **1a** with CO_2 without a catalyst should be kinetically not allowed under mild conditions, as the energy barriers for the carboxylative and intramolecular cyclization steps are high, up to 44.4 and 50.6 kcal mol^{-1}, respectively.

3.2. Catalytic Reaction Mechanism. In Lu's experiment,[9a] the NHO−CO_2 adduct ($ImH_2N^{2,6\text{-}iPr}C_6H_3iPr$) bearing 2,6-diisopropylphenyl and isopropyl groups at the *N*-positions of the imidazolium ring exhibited the highest activity in catalyzing carboxylative cyclization of **1a** with CO_2. Thus, all possible catalytic reaction mechanisms were explored in the presence of this NHO−CO_2 adduct, which is a way to determine the minimum energy reaction pathway (MERP) and the catalytic role of NHO−CO_2 adducts or free NHOs in the reaction. For the sake of brevity, the energetics associated with the two catalytic cycles shown in Scheme 2 are discussed in detail below. The optimized structures and relative energies for the relevant IMs and TSs involved in other mechanisms are provided in the Supporting Information.

3.2.1. Pathway 1: Nucleophilic Addition Mechanism Mediated by the NHO−CO_2 Adduct. The computed potential energy surface (PES) for the nucleophilic addition mediated by the NHO−CO_2 adduct is presented in Figure 2. Along this reaction pathway, a reactant−catalyst molecular complex **1** is initially formed, which lies 6.9 kcal mol^{-1} above the reference energy point. From complex **1**, an intermolecular nucleophilic addition from the carboxylate oxygen anion of the NHO−CO_2 adduct to the C≡C bond of **1a** takes place via $\mathbf{TS_{1-2}}$, pushing more electron density to the terminal carbon atom of the alkynyl group. The relative free energy of $\mathbf{TS_{1-2}}$ is predicted to be 34.7 kcal mol^{-1}, implying that the nucleophilicity of the NHO−CO_2 adduct might be insufficient. In the resultant IM **2**, a large negative charge (−0.61 e) accumulates on the alkenyl carbon anion, making this species unstable in thermodynamics. Subsequently, the hydroxyl hydrogen atom is snatched by the negatively charged alkenyl carbon anion via a five-membered ring $\mathbf{TS_{2-3}}$ (37.5 kcal mol^{-1}) to give an alkoxide anion IM **3** and release a free energy of 11.5 kcal mol^{-1}. Because a strong thermodynamic driving force usually leads to a lower-energy channel for the proton transfer process, a single molecule of substrate **1a** or water-assisted proton transfer from the hydroxyl oxygen atom to the alkenyl carbon anion was further

DOI: 10.1021/acs.joc.6b00559
J. Org. Chem. 2016, 81, 5303−5313

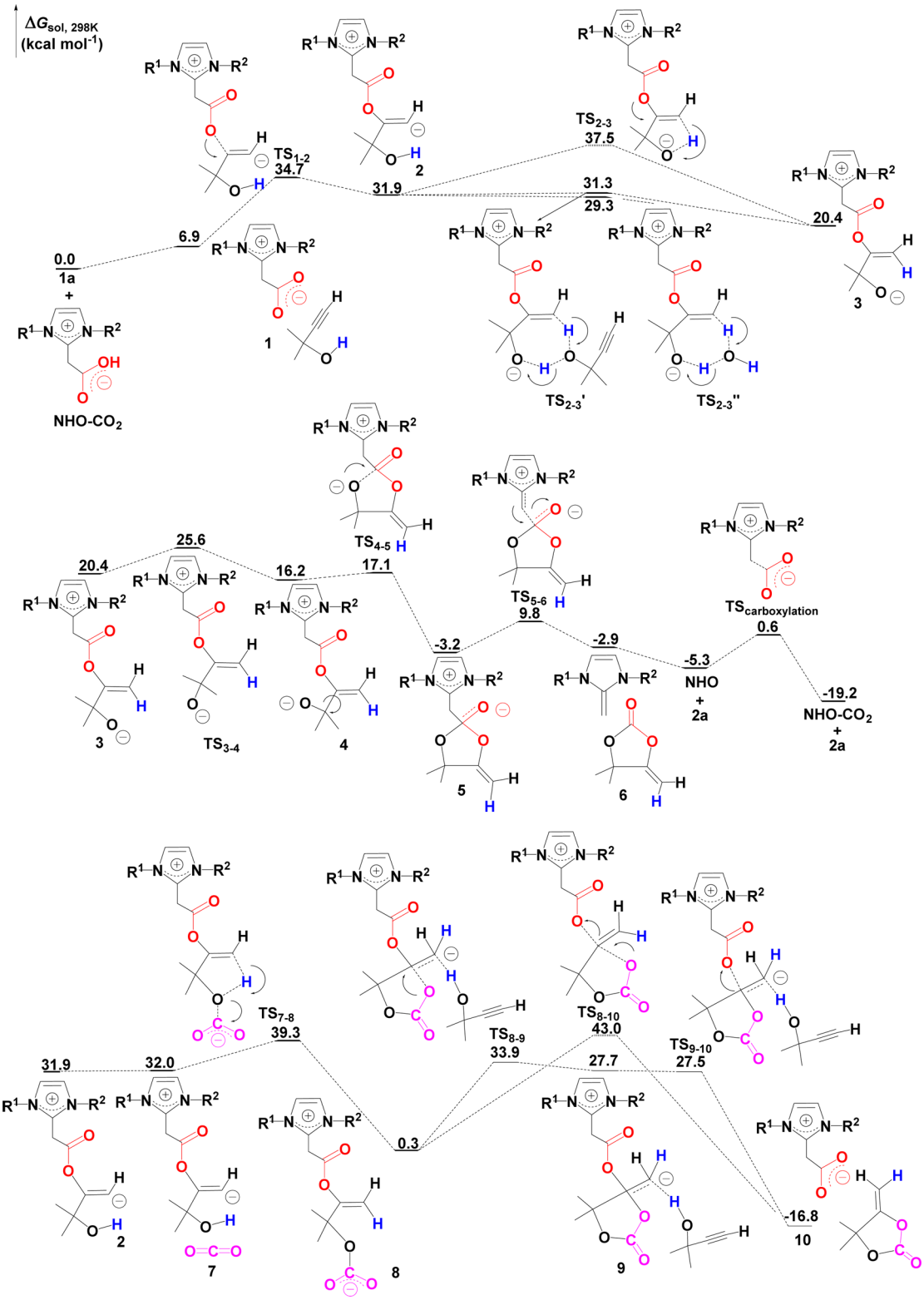

Figure 2. Energy profile for carboxylative cyclization of **1a** with CO_2 along pathway 1 calculated at the M06-2X(SMD, CH_2Cl_2)/6-311++G**//M06-2X(SMD, CH_2Cl_2)/6-31+G* level.

considered, as alcohol and water molecules are well-known proton shuttles in other areas of the proton transfer process.[27] The computed relative free energies of **1a** or water-assisted six-membered ring concerted $\mathbf{TS_{2-3}}'$ and $\mathbf{TS_{2-3}}''$ are 31.3 and 29.3 kcal mol^{-1}, respectively, which is expected to be lower than that of $\mathbf{TS_{2-3}}$. Thus, both **1a** and water could serve as the proton shuttle for accelerating this proton transfer process. From IM **3**, the following isomerization over C−C bond rotation $\mathbf{TS_{3-4}}$ (25.6 kcal mol^{-1}) allows the nucleophilic alkoxide anion facing toward the carboxylate moiety in IM **4**. With this conformation, the intramolecular cyclization with the generation of the **2a**−NHO adduct (IM **5**, −3.2 kcal mol^{-1}) can easily occur through

DOI: 10.1021/acs.joc.6b00559
J. Org. Chem. 2016, 81, 5303−5313

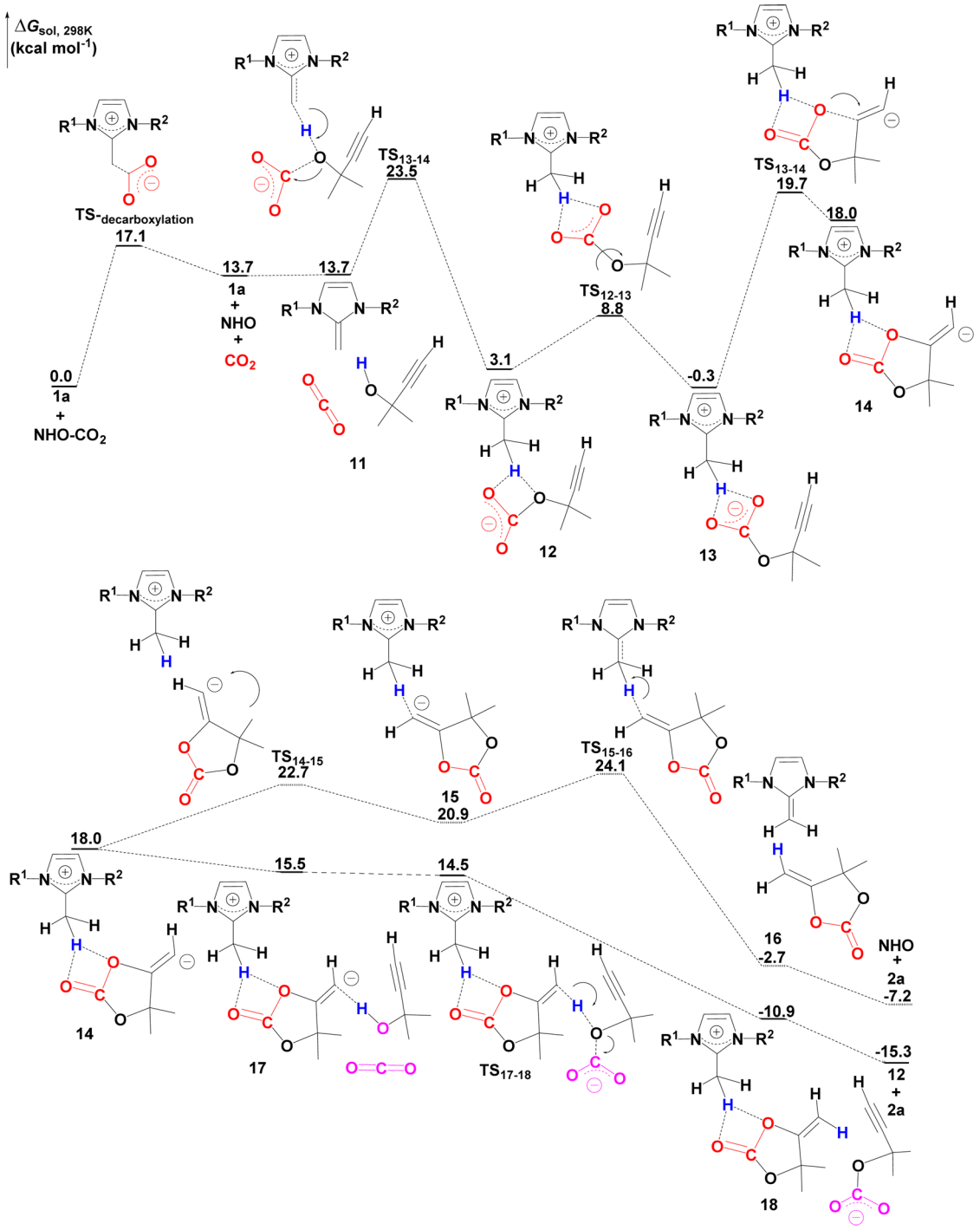

Figure 3. Energy profile for carboxylative cyclization of **1a** with CO_2 along pathway 2 calculated at the M06-2X(SMD, CH_2Cl_2)/6-311++G**//M06-2X(SMD, CH_2Cl_2)/6-31+G* level.

an intramolecular nucleophilic addition $\mathbf{TS}_{4-5}$, with a low energy barrier of 0.9 kcal mol^{-1}. Finally, IM **5** experiences a C−C bond cleavage $\mathbf{TS}_{5-6}$ (9.8 kcal mol^{-1}) to release product **2a** and free NHO, and the subsequent carboxylation of free NHO with CO_2 (TS carboxylation, 0.6 kcal mol^{-1}) will produce the NHO−CO_2 adduct. Alternatively, a branched channel from reactant complex **7** to product−catalyst complex **10** was also considered for the transformation of alkenyl anion IM **2** to product **2a** and the NHO−CO_2 adduct. Along this channel, the proton transfer from the hydroxyl oxygen atom to the alkenyl carbon anion is coupled with the insertion of one molecule of CO_2 into the forming alkoxide oxygen anion, resulting in a carboxylation IM **8**. The free energy barrier for the formation of IM **8** via $\mathbf{TS}_{7-8}$ is predicted to be 39.3 kcal mol^{-1}, which is higher than that of substrate **1a** or the water-assisted proton transfer process. Then, the intramolecular nucleophilic attack from the carboxyl oxygen anion to the sp^2 hybrid alkenyl carbon atom occurs, which leads to the formation of product **2a** and the regeneration of the NHO−CO_2 adduct. For this intramolecular cyclization step, the **1a**-assisted addition−elimination mechanism (**8** → $\mathbf{TS}_{8-9}$ → **9** → $\mathbf{TS}_{9-10}$ → **10**) is found to be kinetically more favorable than the backside S_N2

DOI: 10.1021/acs.joc.6b00559
J. Org. Chem. 2016, 81, 5303−5313

nucleophilic substitution mechanism (**8** → $\mathbf{TS_{8-10}}$ → **10**). Because of the much higher energy barrier requested at $\mathbf{TS_{7-8}}$, this branched channel could be safely ruled out for the whole pathway.

In addition, other nucleophilic addition mechanisms, such as the nucleophilic addition of the NHO−CO_2 adduct to **1a** associated with the insertion of an external molecule of CO_2 into the alkynyl group (pathway 3, Figure S1) and the nucleophilic addition of free NHO to the C≡C bond of **1a** (pathway 4, Figure S2), were computationally examined, as well. Among these three nucleophilic addition mechanisms, the energy height of the highest point (EHHP) at $\mathbf{TS_{1-2}}$ (34.7 kcal mol^{-1}) along pathway 1 is the lowest. Thus, it is clear that pathway 1 should be the MERP for the nucleophilic addition mechanism.

3.2.2. Pathway 2: Basic Ionic Pair Mechanism Mediated by NHO. On the other hand, the basic ionic pair mechanism mediated by NHO was also used for the catalytic reaction. As shown in Figure 3, pathway 2 starts from the decarboxylation of the NHO−CO_2 adduct via a C−C bond cleavage TS, leading to the generation of free NHO and CO_2. The free energy barrier of this decarboxylation step is 17.1 kcal mol^{-1}, and the whole decarboxylation process is endergonic by 13.7 kcal mol^{-1}. These results are quite compatible with the experimental observation that the decomposition of the NHO−CO_2 adduct to free NHO and CO_2 takes place at 40 °C, and the NHO−CO_2 adduct and free NHO are in a dynamic equilibrium.[9a] Next, the resultant NHO and CO_2 molecules approach **1a**, resulting in complex **11**. From this termolecular molecule, the deprotonation of **1a** by free NHO, coupled with the insertion of one molecule of CO_2 with the forming alkoxide oxygen anion, takes place at $\mathbf{TS_{11-12}}$. In comparison with the uncatalyzed carboxylation of **1a** with CO_2 via *b*-**TS1** (44.4 kcal mol^{-1}), the catalytic effect of free NHO is significant, as the relative free energy of $\mathbf{TS_{11-12}}$ is sharply reduced to 23.5 kcal mol^{-1}. Additionally, we also tested the deprotonation of **1a** by free NHO in the absence of CO_2 (see Figure S4). This process needs to overcome a relatively higher energy barrier (24.5 kcal mol^{-1}), suggesting that the concerted carboxylation of **1a** with CO_2 is slightly more favorable in kinetics. After cross $\mathbf{TS_{11-12}}$, an ionic pair IM **12** is formed, in which one hydrogen atom of the $[NHOH]^+$ cation simultaneously interacts with the carboxylate and hydroxyl oxygen atoms of the $[carbonate]^-$ anion. The following isomerization of IM **12** via the C−O bond rotation $\mathbf{TS_{12-13}}$ (8.8 kcal mol^{-1}) makes one of the carboxylate oxygen atoms face toward the alkynyl group. This isomerization also alters the interactions between the $[NHOH]^+$ cation and the $[carbonate]^-$ anion, giving a more stable ionic pair IM **13** (−0.3 kcal mol^{-1}). From IM **13**, the intramolecular nucleophilic addition of the carboxylate oxygen anion to the alkynyl group occurs. The *trans*-conformational $\mathbf{TS_{13-14}}$ (19.7 kcal mol^{-1}) is predicted to be energetically more preferred than analogue $\mathbf{TS_{13-14}}'$ (24.1 kcal mol^{-1}) adopting the *cis* configuration. This result is in good agreement with the X-ray crystal structure determination by Ikariya and co-workers[14d] that *Z*-configurational *α*-alkylidene cyclic carbonates were produced by $P(n\text{-}C_4H_9)_3$-catalyzed carboxylative cyclization of propargyl alcohols with supercritical CO_2. Relative to the uncatalyzed intramolecular cyclization via *b*-**TS3** (50.6 kcal mol^{-1}), the relative free energy of $\mathbf{TS_{13-14}}$ is also remarkably lowered. After the intramolecular cyclization, ring-closed carbonate IM **14** (18.0 kcal mol^{-1}) is formed, in which the large negative charge (−0.60 e) accumulates on the alkenyl carbon anion, as well. From IM **14**, two scenarios for the protonation of the alkenyl carbon anion are possible, because the $[NHOH]^+$ cation and excess **1a** are both available proton sources in the reaction system. To complete the protonation of the alkenyl carbon anion with the $[NHOH]^+$ cation, the cyclic carbonate moiety in IM **14** first needs to undergo a conformational rotation $\mathbf{TS_{14-15}}$ (22.7 kcal mol^{-1}), permitting the alkenyl carbon anion to orient toward the methyl group of the $[NHOH]^+$ cation in IM **15**. Then, the migration of hydrogen from the $[NHOH]^+$ cation to the alkenyl carbon anion proceeds through a C−H bond cleavage $\mathbf{TS_{15-16}}$ (24.1 kcal mol^{-1}), leaving a product−catalyst complex **16** (−2.7 kcal mol^{-1}) behind. The isolation of **2a** from complex **16** recovers free NHO and completes the catalytic cycle shown in Scheme 2. Alternatively, when an external molecule **1a** is employed as the proton donor, the interaction of the hydroxyl group of **1a** with the alkenyl carbon anion of IM **14** forms a molecular complex **17**. In this complex, the negative charge on the alkenyl carbon anion is delocalized by the hydroxyl group of **1a**, and thus, the relative free energy of complex **17** is reduced by 2.9 kcal mol^{-1} relative to that of IM **14**. Meanwhile, the O−H bond in complex **17** is weakened, as reflected by the smaller Wiberg bond index (0.472 vs 0.771 in **1a**). Consequently, the subsequent proton transfer from the hydroxyl group of **1a** to the alkenyl carbon anion can easily occur, which is associated with the insertion of one molecule of CO_2 with the forming alkoxide oxygen anion, leading to a product−catalyst complex **18** (−10.9 kcal mol^{-1}). Although the computed relative energy of $\mathbf{TS_{17-18}}$ is slightly lower than that of complex **17** by 1.0 kcal mol^{-1}, the vibration frequency calculation confirms that $\mathbf{TS_{17-18}}$ is a first-order saddle point with a unique imaginary frequency of −760.0 cm^{-1}. This result is similar to the theoretical calculations of the proton transfer processes, suggesting that the PES around this area is very flat.[28] Finally, the separation of **2a** from complex **18** will regenerate IM **12**. From Figure 3, it is apparent that the protonation of IM **14** with **1a** is kinetically and thermodynamically more preferable than that with the $[NHOH]^+$ cation. The reason might be that the cleavage of the O−H bond in **1a** is more feasible than that of the C−H bond in the $[NHOH]^+$ cation. As a result, the catalytic cycle of this basic ionic pair mechanism should be composed of three elementary steps: (i) isomerization of ionic pair IM **12** to IM **13**, (ii) intramolecular nucleophilic cyclization of IM **13**, leading to alkenyl carbon anion IM **14**, and (iii) protonation of IM **14** with **1a** to yield product **2a** and regenerate IM **12**. The free NHO primarily acts as a strong base to trigger the generation of $[NHOH]^+[carbonate]^-$ ionic pair IM **12** in the carboxylation of **1a** with CO_2.

Moreover, it should be mentioned that the other analogue basic ionic pair mechanism by employing the NHO−CO_2 adduct as the basic promoter was also comparatively studied (pathway 5, Figure S3). The calculations show that the deprotonation and carboxylation of **1a** with CO_2 promoted by the NHO−CO_2 adduct are more facile, with a low energy barrier of 8.4 kcal mol^{-1}. However, the computed EHHP of 28.3 kcal mol^{-1} at the protonation step along this pathway is much higher than that in pathway 2. Thus, this ionic pair mechanism could be excluded, as well.

So far, the overall mechanism of the catalytic reaction is clear. For the nucleophilic addition mechanism along pathway 1, an EHHP of 34.7 kcal mol^{-1} is required at $\mathbf{TS_{1-2}}$, while a much lower one of 23.5 kcal mol^{-1} at $\mathbf{TS_{11-12}}$ is predicted for the basic ionic pair mechanism along pathway 2. The computed

DOI: 10.1021/acs.joc.6b00559
J. Org. Chem. 2016, 81, 5303−5313

EHHP of 23.5 kcal mol^{-1} also qualitatively agrees with the experimental observations that the reaction could proceed at a temperature of 60 °C and a CO_2 pressure of 2.0 MPa within 12 h.[9a] Therefore, we can conclude that the carboxylative cyclization of **1a** with CO_2 in the presence of the NHO−CO_2 adduct should adopt the NHO-mediated basic ionic pair mechanism rather the nucleophilic addition mechanism being catalyzed by the NHO−CO_2 adduct. For the NHO-mediated basic ionic pair mechanism, [NHOH]$^+$[carbonate]$^-$ ion pair IM **13** and intramolecular cyclization $\mathbf{TS_{13-14}}$ can be regarded as the turnover frequency intermediate (TDI[29]) and turnover frequency transition state (TDTS) in the catalytic cycle, respectively. The global energy span between the TDI and TDTS is 20.0 kcal mol^{-1}, and the turnover frequency (TOF[29]) value of the catalytic cycle is calculated to be 4.9 × 10 h^{-1}. These computed values are also in good agreement with the experimental result that the product **2a** could be obtained in high yield (up to 98%) within the short period of reaction time (12 h).[9a] In addition, the rate constants for the two crucial steps (k_1 for **1a** + NHO−CO_2 → $\mathbf{TS_{11-12}}$ and k_2 for IM **13** → $\mathbf{TS_{13-14}}$) were also quantitatively estimated according to the conventional transition state theory,[30a] including the tunneling correction.[30b] Over the temperature range of 278−328 K, the rate constants can be fitted by the following expressions: $k_1(T)$ (in moles per cubic decimeter per second) = 2.899 × 10^6 exp(−59252/RT) and $k_2(T)$ (in inverse seconds) = 6.547 × 10^{12} exp(−82470/RT) (see section S4 of the Supporting Information for calculation details).

3.3. More Insights into the NHO Organocatalyst. Our understanding of catalytic reaction mechanisms motivated us to gain more insights into the catalytic activity of NHOs because of their great catalytic potential in promoting CO_2 fixation reactions.

3.3.1. Why Is the Basic Ionic Pair Mechanism More Preferred Than the Nucleophilic Addition Mechanism? According to the relevant literature[7,9a] as well as the results of chemical reactivity index analysis[31,32] (Table 1), both the NHO−CO_2 adduct and free NHO can be considered as strong nucleophiles (N > 3.0 eV).[33] However, DFT calculations of the catalytic reaction suggest that the intermolecular nucleophilic addition from the NHO−CO_2 adduct or free NHO to the C≡C bond of **1a** requires a high EHHP of 34.7 or 39.9 kcal mol^{-1}, respectively. In contrast, the deprotonation of **1a** by the NHO−CO_2 adduct or free NHO is relatively more facile, with a much lower EHHP of 8.4 or 23.5 kcal mol^{-1}, respectively. To explain these computed results, molecular orbital (MO) and nature population analysis (NPA) were performed on substrate **1a**, the NHO−CO_2 adduct, and free NHO.

Table 1. Electronic Chemical Potentials (μ), Chemical Hardnesses (η), Global Electrophilicities (ω), and Global Nucleophilicities (N) (all in electronvolts) for the Selected Reactants, Catalysts, and IMs Calculated at the M062x/6-311++G Level**

	μ	η	ω	N
CO_2	−12.4	12.3	6.3	−1.5
1a	−9.3	9.0	4.8	1.7
NHO−CO_2	−7.8	6.6	4.7	3.7
NHO	−5.6	5.3	3.0	5.4
[NHOH]$^+$[carbonate]$^-$ **13**	−7.8	6.6	4.6	3.7
[NHOH]$^+$	−14.3	7.9	13.1	−0.2
[carbonate]$^-$	−1.0	5.8	0.1	7.5

From MO analysis (Figure 4), it is clear that the LUMO of **1a** is predominantly contributed by the s orbital of the hydroxyl hydrogen atom while the LUMO+1 orbital of **1a** is mainly contributed by the empty π orbital of the alkynyl group. Hence, the charge transfer from the p orbital of the carboxylate oxygen anion in the HOMO of the NHO−CO_2 adduct or the p orbital of the α-carbon atom in the HOMO of free NHO to the empty π orbital of the alkynyl group in the LUMO+1 orbital of **1a** needs to overcome a greater energy gap (~10.3 kcal mol^{-1} for the energy gap between LUMO+1 and LUMO of **1a**). On the other hand, the NPA charge analysis (Scheme 3) shows that the middle carbon atom of the alkynyl group is negatively charged in **1a**, which may not prefer to accept the nucleophilic attack from the negatively charged carboxylate oxygen anion in the NHO−CO_2 adduct or the α-carbon atom in free NHO. On the contrary, the hydroxyl hydrogen atom with the positive charge has good affinity for the carboxylate oxygen anion in the NHO−CO_2 adduct or the α-carbon atom in free NHO. Therefore, the activation energy barrier for the deprotonation

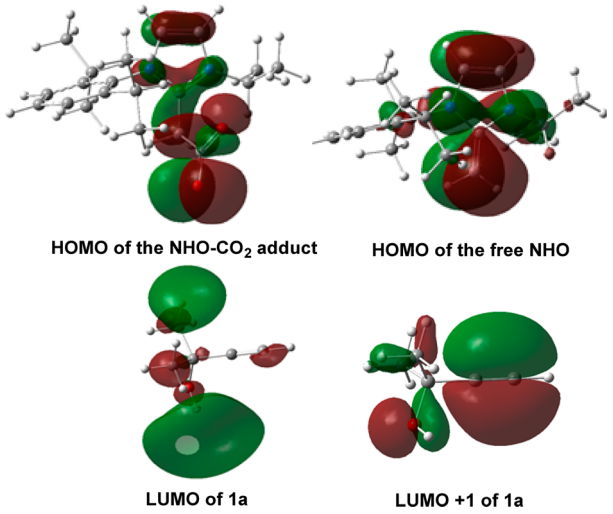

Figure 4. Visualization of the selected molecular orbitals of the NHO−CO_2 adduct, free NHO, and propargyl alcohol **1a**.

Scheme 3. NPA Charges of the Key Species Labeled in Red (positive) and Blue (negative)

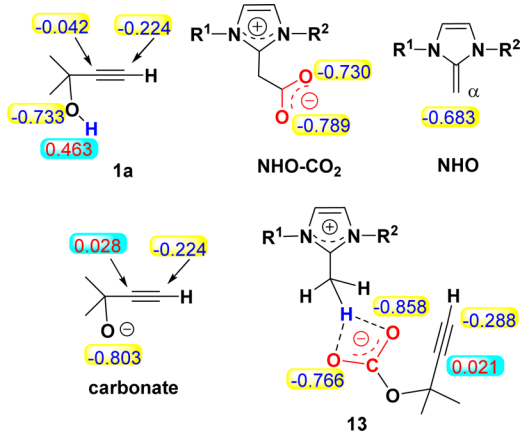

DOI: 10.1021/acs.joc.6b00559
J. Org. Chem. 2016, 81, 5303−5313

of **1a** by the NHO−CO_2 adduct or free NHO is calculated to be much lower. Furthermore, we also notice that the NPA charge on the middle carbon atom of the alkynyl group becomes positive in the carbonate anion or $[NHOH]^+[carbonate]^-$ ionic pair IM **13**, and the terminal carbon atom is more negatively charged. In other words, π bonds of the alkenyl group are polarized to some extent in these species, which are certainly more susceptible to accepting a nucleophilic attack from the carbonate oxygen anion, leading to the preference for the intramolecular cyclization step.

3.3.2. How Does the Substituent Effect of NHOs Influence the Catalytic Reaction? Similar to those of NHCs,[11a,b,34a] the thermal stability of NHO−CO_2 adducts and the catalytic activity of NHOs are also related to the electronic and steric effect of *N*- and *C*-substituents on the imidazolium ring.[9a] Herein, four sets of NHOs (in Scheme 4) were employed to simulate the catalytic reaction, with the aim of clarifying the substituent effect of NHOs on the catalytic reaction. The free NHO ($ImH_2N^{2,6\text{-}iPr}C_6H_3iPr$) used in the mechanistic study was chosen as the reference system. As mentioned above, the catalytic cycle is triggered by the formation of $[NHOH]^+[carbonate]^-$ IM **12** through NHO-mediated carboxylation of **1a** with CO_2, which is the initial reaction rate that is influenced by the EHHP of $\mathbf{TS}_{11-12}$ ($\Delta G_1^{\ddagger}$) relative to the separated NHO−CO_2 adduct and **1a**. After this energy summit has been crossed, the catalytic cycle can proceed. IM **13** and $\mathbf{TS}_{13-14}$ in the intramolecular step are TDI and TDTS in the catalytic cycle, respectively, meaning that the TOF value is dependent on the global energy span ($\Delta G_2^{\ddagger}$) between IM **13** and $\mathbf{TS}_{13-14}$. Accordingly, the values of $\Delta G_1^{\ddagger}$ and $\Delta G_2^{\ddagger}$ for these two crucial steps (**1a** + NHO−CO_2 → $\mathbf{TS}_{11-12}$ and IM **13** → $\mathbf{TS}_{13-14}$) were calculated at the same level of theory. Because NHO−CO_2 adducts, free NHOs, and CO_2 molecules are generally in reversible equilibria and NHO−CO_2 adducts are more thermodynamically stable, the sum of free energies of NHO−CO_2 adducts and **1a** is set as the energy point reference.

Initially, the effect of *C*-substituents on the catalytic reaction was investigated (sets A and B). The relationship between substituent R^1 groups and free energy barriers in carboxylative and intramolecular steps is depicted in panels a and b of Figure 5, respectively. In the case of set A, the value of $\Delta G_1^{\ddagger}$ is gradually increased when the electron-withdrawing group is replaced with the electron-donating one. This result means that the introduction of electron-withdrawing groups at the *C*-positions of the imidazolium ring will accelerate the catalytic carboxylation of **1a** with CO_2. The reason might be attributed to the weak nucleophilicity of free NHO that bears the electron-withdrawing *C*-substituent.[23] In other words, the electron-withdrawing *C*-substituent can inhibit the competing side reaction (NHO + CO_2 → NHO−CO_2), leading to the preference for the desired carboxylation of **1a** with CO_2. However, the value of $\Delta G_2^{\ddagger}$ is also increased when the electron-withdrawing effect of the R^1 group is enhanced. This might be due to the fact that the stabilization interaction from the $[NHOH]^+$ cation to the $[carbonate]^-$ anion is looser (see section S5 of the Supporting Information for the characterization of stabilization interactions between the $[NHOH]^+$ cation and the $[carbonate]^-$ anion). Because the higher value of $\Delta G_2^{\ddagger}$ will lead to the lower TOF, the introduction of electron-withdrawing groups at the *C*-positions of the imidazolium ring might reduce the catalytic efficiency of NHOs. For set B, the trend for the value of $\Delta G_1^{\ddagger}$ is also monotonically increased when the electron-donating effect of the *C*-substituent is increased. The computed absolute values of $\Delta G_1^{\ddagger}$ in set B are lower, which might be due to the effect of the *N*-substituent. The trend for the values of $\Delta G_2^{\ddagger}$ is not very regular, but it is general smoothly decreased like that in set A, except for the NHO with the -CO_2Me group. On the basis of the results described above, we can predict that the catalytic effect of NHOs may not be improved by tuning the electronic effect of the *C*-substituent on the imidazolium ring.

Next, the effect of *N*-substituents was explored (set C). As shown in Figure 5c, the values of $\Delta G_1^{\ddagger}$ and $\Delta G_2^{\ddagger}$ are gradually reduced when the electron-donating effect of the R^2 group is increased. These results suggest that the *N*-substituents have an obvious influence on catalyst activity. The *N*-substituents with the strong electron-withdrawing effect will seriously reduce the proton affinity of free NHOs and weaken the stabilization between the $[NHOH]^+$ cation and the $[carbonate]^-$ anion and thus disfavor both carboxylative and intramolecular processes. Relative to NHOs substituted with methyl and isopropyl groups, the form substituted with a *tert*-butyl group has a better catalytic effect on both carboxylative and intramolecular cyclization steps, which might be due to the stronger electron-donating effect and bulkier steric effect of the *tert*-butyl group. The strong electron-donating effect will enhance the proton affinity of the α-carbon atom, while the bulky steric effect will inhibit the competing capture of CO_2 with the formation of the NHO−CO_2 adduct, making the catalytic carboxylation of **1a** with CO_2 faster. Meanwhile, *tert*-butyl groups with the stronger electron-donating effect also favor stabilization of the carbonate anion. Thus, the computed $\Delta G_2^{\ddagger}$ value of 20.0 kcal mol^{-1} is comparable with that of the reference system. On the other hand, the computed $\Delta G_2^{\ddagger}$ values of 22.6 and 21.9 kcal mol^{-1} for methyl- and isopropyl-substituted NHOs are higher, which is also in line with the experimental observations that **2a** was obtained in lower yields (51 and 72%) when methyl and isopropyl groups are introduced at the *N*-positions of the imidazolium ring, respectively.[9a] The results described above indicate that both the electronic effect and the steric effect will influence the catalytic activity of NHOs.

Finally, the catalytic effect of NHOs bearing saturated or unsaturated rings fused at the *N*- and *C*-positions was examined (set D). Among these four free NHOs, ImDpylm NHO gives the satisfactory catalytic effect on both carboxylative ($\Delta G_1^{\ddagger}$ = 19.8 kcal mol^{-1}) and intramolecular cyclization ($\Delta G_2^{\ddagger}$ = 20.4 kcal mol^{-1}) processes. This result might be attributed to the sp^2-hybridized carbon atoms as the weak electron-withdrawing

Scheme 4. Selected NHOs with Typical Abbreviations[34b] in a Simulation of the Carboxylative Cyclization of 1a with CO_2

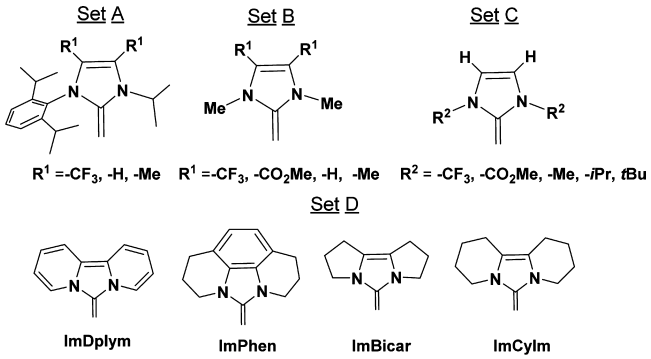

DOI: 10.1021/acs.joc.6b00559
J. Org. Chem. 2016, 81, 5303−5313

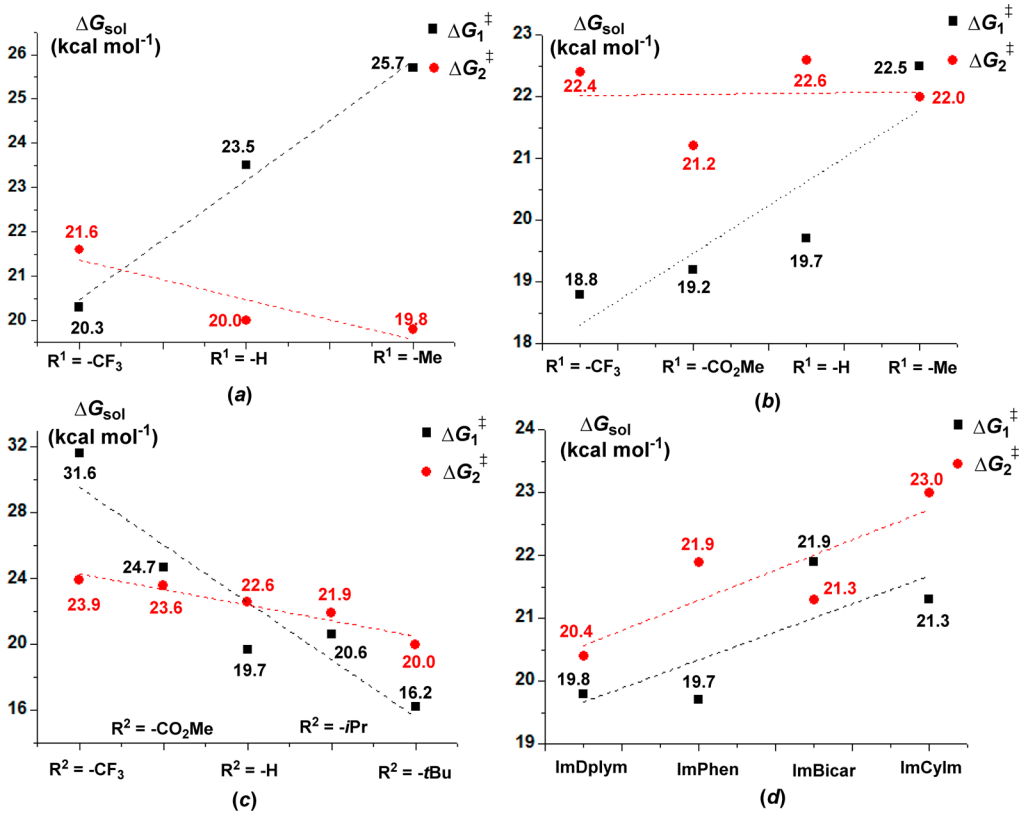

Figure 5. Relationship between substituents of NHOs and free energy barriers ($\Delta G_1^{\ddagger}$ and $\Delta G_2^{\ddagger}$) in steps of carboxylation of **1a** with CO_2 and intramolecular cyclization of IM **13**.

groups have a small impact on the proton affinity of the α-carbon atom in NHO and the stabilization interaction between the $[NHOH]^+$ cation and the $[carbonate]^-$ anion.

4. CONCLUSIONS

The catalytic mechanism of NHO organocatalysts in the carboxylative cyclization reaction of propargyl alcohol with CO_2 has been comprehensively investigated with DFT calculations. The major conclusions are as follows.

The calculations reveal that the catalytic reaction prefers to proceed via the NHO-mediated basic ionic pair mechanism rather than the nucleophilic addition mechanism being catalyzed by the NHO−CO_2 adduct. Thus, the NHO−CO_2 adduct with the lower thermostability for easily releasing free NHO should be chosen as the catalytic precursor for the reaction. The free NHO primarily plays as a basic promoter to trigger the carboxylative of propargyl alcohol with CO_2, leading to the formation of the $[NHOH]^+[carbonate]^-$ ion pair intermediate. Once this active species is generated, the catalytic cycle can easily proceed, including isomerization of the $[NHOH]^+[carbonate]^-$ ion pair intermediate, intramolecular nucleophilic attack of the oxygen anion on the alkynyl group, and transfer of a proton from the external molecule propargyl alcohol to the alkenyl anion intermediate.

MO and NPA charge analysis discloses that the preference for the basic ionic pair mechanism is due to the favorable orbital and charge interactions between the α-carbon atom of NHO and the hydroxyl hydrogen atom of propargyl alcohol. In other words, the basicity of the catalyst rather than its nucleophilicity should be considered to be more significant for this kind of reaction.

The investigations of the substituent effect of NHOs show that *N*-substituents with a large electron donating and bulky steric effect are crucial for the catalytic activity of NHOs, which may assist the experimenters in further modifying NHO organocatalysts.

■ ASSOCIATED CONTENT

Supporting Information

The Supporting Information is available free of charge on the ACS Publications website at DOI: 10.1021/acs.joc.6b00559.

Computational details, optimized geometries, calculated energies, and the full citation of Gaussian 09 (PDF)

■ AUTHOR INFORMATION

Corresponding Author

*School of Science, Xihua University, Chengdu, Sichuan 610039, P. R. China. E-mail: weiyili@mail.xhu.edu.cn. Telephone: +86-028-87727663. Fax: +86-028-87727663.

Notes

The authors declare no competing financial interest.

■ ACKNOWLEDGMENTS

The authors are grateful for the financial support from the National Natural Science Foundation of China (21402158), the Scientific Research Fund of the Education Department of Sichuan Province (14ZB0131), the Key Scientific Research Fund (Z1313319), and the Open Research Subject of Key Laboratory (Research center for advanced computation) of Xihua University (szjj2015-051).

DOI: 10.1021/acs.joc.6b00559
J. Org. Chem. 2016, 81, 5303−5313

REFERENCES

(1) (a) Berkefeld, A.; Piers, W. E.; Parvez, M. *J. Am. Chem. Soc.* **2010**, *132*, 10660−10661. (b) Mitton, S. J.; Turculet, L. *Chem. - Eur. J.* **2012**, *18*, 15258−15262. (c) LeBlanc, F. A.; Piers, W. E.; Parvez, M. *Angew. Chem., Int. Ed.* **2014**, *53*, 789−792. (d) Courtemanche, M.-A.; Légaré, M.-A.; Rochette, É.; Fontaine, F.-G. *Chem. Commun.* **2015**, *51*, 6858−6861.

(2) (a) Han, Z.; Rong, L.; Wu, J.; Zhang, L.; Wang, Z.; Ding, K. *Angew. Chem., Int. Ed.* **2012**, *51*, 13041−13045. (b) Courtemanche, M.-A.; Légaré, M.-A.; Maron, L.; Fontaine, F.-G. *J. Am. Chem. Soc.* **2013**, *135*, 9326−9329. (c) Courtemanche, M.-A.; Légaré, M.-A.; Maron, L.; Fontaine, F.-G. *J. Am. Chem. Soc.* **2014**, *136*, 10708−10717. (d) Rezayee, N. M.; Huff, C. A.; Sanford, M. S. *J. Am. Chem. Soc.* **2015**, *137*, 1028−1031. (e) Chong, C. C.; Kinjo, R. *ACS Catal.* **2015**, *5*, 3238−3259.

(3) (a) Nair, V.; Varghese, V.; Paul, R. R.; Jose, A.; Sinu, C. R.; Menon, R. S. *Org. Lett.* **2010**, *12*, 2653−2655. (b) Yu, D.; Zhang, Y. *Green Chem.* **2011**, *13*, 1275−1279. (c) Fujihara, T.; Nogi, K.; Xu, T.; Terao, J.; Tsuji, Y. *J. Am. Chem. Soc.* **2012**, *134*, 9106−9109. (d) Shintani, R.; Nozaki, K. *Organometallics* **2013**, *32*, 2459−2462.

(4) (a) Song, Q.; He, L.; Wang, J.; Yasuda, H.; Sakakura, T. *Green Chem.* **2013**, *15*, 110−115. (b) Ren, Y.; Shim, J. J. *ChemCatChem* **2013**, *5*, 1344−1349. (c) Monassier, A.; D'Elia, V.; Cokoja, M.; Dong, H.; Pelletier, J. D. A.; Basset, J. M.; Kühn, F. E. *ChemCatChem* **2013**, *5*, 1321−1324. (d) Castro-Gómez, F.; Salassa, G.; Kleij, A. W.; Bo, C. *Chem. - Eur. J.* **2013**, *19*, 6289−6298. (e) Anthofer, M. H.; Wilhelm, M. E.; Cokoja, M.; Markovits, I. I. E.; Pöthig, A.; Mink, J.; Herrmann, W. A.; Kühn, F. E. *Catal. Sci. Technol.* **2014**, *4*, 1749−1758. (f) Luo, R.; Zhou, X.; Fang, Y. X.; Ji, H. *Carbon* **2015**, *82*, 1−11. (g) Martín, C.; Fiorani, G.; Kleij, A. W. *ACS Catal.* **2015**, *5*, 1353−1370. (h) Maeda, C.; Taniguchi, T.; Ogawa, K.; Ema, T. *Angew. Chem., Int. Ed.* **2015**, *54*, 134−138. (i) Ma, R.; He, L.-N.; Zhou, Y.-B. *Green Chem.* **2016**, *18*, 226−231.

(5) (a) Sakakura, T.; Choi, J. C.; Yasuda, H. *Chem. Rev.* **2007**, *107*, 2365−2387. (b) Riduan, S. N.; Zhang, Y. *Dalton Trans.* **2010**, *39*, 3347−3357. (c) Aresta, M.; Dibenedetto, A. *Dalton Trans.* **2010**, *39*, 2975−2992. (d) Darensbourg, D. J. *Inorg. Chem.* **2010**, *49*, 10765−10780. (e) Omae, I. *Coord. Chem. Rev.* **2012**, *256*, 1384−1405. (f) Lu, X.-B.; Darensbourg, D. *Chem. Soc. Rev.* **2012**, *41*, 1462−1484. (g) Lu, X. B.; Ren, W. M.; Wu, G. P. *Acc. Chem. Res.* **2012**, *45*, 1721−1735. (h) Tlili, A.; Blondiaux, E.; Frogneux, X.; Cantat, T. *Green Chem.* **2015**, *17*, 157−168.

(6) Crocker, R. D.; Nguyen, T. V. *Chem. - Eur. J.* **2016**, *22*, 2208−2213.

(7) Fürstner, A.; Alcarazo, M.; Goddard, R.; Lehmann, C. W. *Angew. Chem., Int. Ed.* **2008**, *47*, 3210−3214.

(8) (a) Kuhn, N.; Bohnen, H.; Kreutzberg, J.; Blaeser, D.; Boese, R. *J. Chem. Soc., Chem. Commun.* **1993**, 1136−1137. (b) Kuhn, N.; Bohnen, H.; Blaeser, D.; Boese, R. *Chem. Ber.* **1994**, *127*, 1405−1407. (c) Schumann, H.; Glanz, M.; Winterfeld, J.; Hemling, H.; Kuhn, N.; Bohnen, H.; Blaeser, D.; Boese, R. *J. Organomet. Chem.* **1995**, *493*, C14−C18. (d) Kunz, D.; Johnsen, E. O.; Monsler, B.; Rominger, F. *Chem. - Eur. J.* **2008**, *14*, 10909−10914. (e) Ibrahim Al-Rafia, S. M.; Malcolm, A. C.; Liew, S. K.; Ferguson, M. J.; McDonald, R.; Rivard, E. *Chem. Commun.* **2011**, *47*, 6987−6989. (f) Glöckner, A.; Kronig, S.; Bannenberg, T. C.; Daniliuc, G.; Jones, P. G.; Tamm, M. *J. Organomet. Chem.* **2013**, *723*, 181−187. (g) Kronig, S.; Jones, P. G.; Tamm, M. *Eur. J. Inorg. Chem.* **2013**, *2013*, 2301−2314. (h) Iglesias, M.; Iturmendi, A.; Sanz Miguel, P. S.; Polo, V.; Perez-Torrente, J. J.; Oro, L. A. *Chem. Commun.* **2015**, *51*, 12431−12434.

(9) (a) Wang, Y.-B.; Wang, Y.-M.; Zhang, W.-Z.; Lu, X.-B. *J. Am. Chem. Soc.* **2013**, *135*, 11996−12003. (b) Jia, Y.-B.; Wang, Y.-B.; Ren, W.-M.; Xu, T.; Wang, J.; Lu, X.-B. *Macromolecules* **2014**, *47*, 1966−1972. (c) Wang, Y.-B.; Sun, D.-S.; Zhou, H.; Zhang, W.-Z.; Lu, X.-B. *Green Chem.* **2015**, *17*, 4009−4015.

(10) (a) Aresta, M.; Nobile, C. F.; Albano, V. G.; Forni, E.; Manassero, M. *J. Chem. Soc., Chem. Commun.* **1975**, *0*, 636−637. (b) Aresta, M.; Nobile, C. F. *J. Chem. Soc., Dalton Trans.* **1977**, 708−711. (c) Gambarotta, S.; Arena, F.; Floriani, C.; Zanazzi, P. F. *J. Am. Chem. Soc.* **1982**, *104*, 5082−5092. (d) Calabrese, J. C.; Herskovitz, T.; Kinney, J. B. *J. Am. Chem. Soc.* **1983**, *105*, 5914−5915.

(11) (a) Zhou, H.; Zhang, W.; Liu, C.; Qu, J.; Lu, X. *J. Org. Chem.* **2008**, *73*, 8039−8044. (b) Van Ausdall, B. R.; Glass, J. L.; Wiggins, K. M.; Aarif, A. M.; Louie, J. *J. Org. Chem.* **2009**, *74*, 7935−7942. (c) Yang, L.; Wang, H. *ChemSusChem* **2014**, *7*, 962−998. (d) Villiers, C.; Dognon, J. P.; Pollet, R.; Thuéry, P.; Ephritikhine, M. *Angew. Chem., Int. Ed.* **2010**, *49*, 3465−3468.

(12) (a) Toullec, P.; Carbayo Martin, A.; Gio-Batta, M.; Bruneau, C.; Dixneuf, P. H. *Tetrahedron Lett.* **2000**, *41*, 5527−5531. (b) Ochiai, B.; Endo, T. *Prog. Polym. Sci.* **2005**, *30*, 183−215.

(13) (a) Sasaki, Y. *Tetrahedron Lett.* **1986**, *27*, 1573−1574. (b) Inoue, Y.; Ishikawa, J.; Taniguchi, M.; Hashimoto, H. *Bull. Chem. Soc. Jpn.* **1987**, *60*, 1204−1206. (c) Gu, Y.; Shi, F.; Deng, Y. *J. Org. Chem.* **2004**, *69*, 391−394. (d) Jiang, H.-F.; Wang, A.-Z.; Liu, H.-L.; Qi, C.-R. *Eur. J. Org. Chem.* **2008**, *2008*, 2309−2312. (e) Uemura, K.; Kawaguchi, T.; Takayama, H.; Nakamura, A.; Inoue, Y. *J. Mol. Catal. A: Chem.* **1999**, *139*, 1−9. (f) Yamada, W.; Sugawara, Y.; Cheng, H. M.; Ikeno, T.; Yamada, T. *Eur. J. Org. Chem.* **2007**, *2007*, 2604−2607. (g) Yoshida, S.; Fukui, K.; Kikuchi, S.; Yamada, T. *J. Am. Chem. Soc.* **2010**, *132*, 4072−4073.

(14) (a) Fournier, J.; Bruneau, C.; Dixneuf, P. H. *Tetrahedron Lett.* **1989**, *30*, 3981−3982. (b) Joumier, J. M.; Fournier, J.; Bruneau, C.; Dixneuf, P. H. *J. Chem. Soc., Perkin Trans. 1* **1991**, 3271−3274. (c) Joumier, J. M.; Bruneau, C.; Dixneuf, P. H. *Synlett* **1992**, *1992*, 453−454. (d) Kayaki, Y.; Yamamoto, M.; Ikariya, T. *J. Org. Chem.* **2007**, *72*, 647−649.

(15) Della Ca', N.; Gabriele, B.; Ruffolo, G.; Veltri, L.; Zanetta, T.; Costa, M. *Adv. Synth. Catal.* **2011**, *353*, 133−146.

(16) (a) Tommasi, I.; Sorrentino, F. *Tetrahedron Lett.* **2009**, *50*, 104−107. (b) Kayaki, Y.; Yamamoto, M.; Ikariya, T. *Angew. Chem., Int. Ed.* **2009**, *48*, 4194−4197.

(17) Zhou, H.; Wang, G.-X.; Zhang, W.-Z.; Lu, X.-B. *ACS Catal.* **2015**, *5*, 6773−6779.

(18) (a) Huang, F.; Lu, G.; Zhao, L.; Li, H.; Wang, Z. *J. Am. Chem. Soc.* **2010**, *132*, 12388−12396. (b) Ren, X.; Yuan, Y.; Ju, Y.; Wang, H. *ChemCatChem* **2012**, *4*, 1943−1951. (c) Ajitha, M. J.; Suresh, C. H. *Tetrahedron Lett.* **2011**, *52*, 5403−5406. (d) Wang, B.; Cao, Z. *RSC Adv.* **2013**, *3*, 14007−14015. (e) Riduan, S. N.; Ying, J. Y.; Zhang, Y. *ChemCatChem* **2013**, *5*, 1490−1496. (f) Li, W.; Huang, D.; Lv, Y. *RSC Adv.* **2014**, *4*, 17236−17244. (g) Zhou, Q.; Li, Y. *J. Am. Chem. Soc.* **2015**, *137*, 10182−10189.

(19) Frisch, M. J.; et al. *Gaussian 09*, revision A.02; Gaussian, Inc.: Wallingford, CT, 2009.

(20) (a) Zhao, Y.; Truhlar, D. G. *Theor. Chem. Acc.* **2008**, *120*, 215−241. (b) Zhao, Y.; Truhlar, D. G. *Acc. Chem. Res.* **2008**, *41*, 157−167.

(21) (a) Ditchfield, R.; Hehre, W. J.; Pople, J. A. *J. Chem. Phys.* **1971**, *54*, 724−728. (b) Hehre, W. J.; Ditchfield, R.; Pople, J. A. *J. Chem. Phys.* **1972**, *56*, 2257−2261. (c) Hariharan, P. C.; Pople, J. A. *Mol. Phys.* **1974**, *27*, 209−214.

(22) Marenich, A. V.; Cramer, C. J.; Truhlar, D. G. *J. Phys. Chem. B* **2009**, *113*, 6378−6396.

(23) Dong, L.; Wen, J.; Li, W. *Org. Biomol. Chem.* **2015**, *13*, 8533−8544.

(24) (a) Fukui, K. *J. Phys. Chem.* **1970**, *74*, 4161−4163. (b) Fukui, K. *Acc. Chem. Res.* **1981**, *14*, 363−368.

(25) (a) Benson, S. W. *The Foundations of Chemical Kinetics*; Krieger: Malabar, FL, 1982. (b) Okuno, Y. *Chem. - Eur. J.* **1997**, *3*, 212−218. (c) Ardura, D.; López, R.; Sordo, T. L. *J. Phys. Chem. B* **2005**, *109*, 23618−23623. (d) Schoenebeck, F.; Houk, K. N. *J. Am. Chem. Soc.* **2010**, *132*, 2496−2497.

(26) (a) Reed, A. E.; Weinhold, F. *J. Chem. Phys.* **1985**, *83*, 1736−1740. (b) Reed, A. E.; Weinstock, R. B.; Weinhold, F. *J. Chem. Phys.* **1985**, *83*, 735−746. (c) Reed, A. E.; Curtiss, L. A.; Weinhold, F. *Chem. Rev.* **1988**, *88*, 899−926. (d) Reed, A. E.; Schleyer, P. R. *J. Am. Chem. Soc.* **1990**, *112*, 1434−1445.

(27) (a) Krauter, C. M.; Hashmi, A. S. K.; Pernpointner, M. *ChemCatChem* **2010**, *2*, 1226−1230. (b) Roy, D.; Patel, C.; Sunoj, R. B. *J. Org. Chem.* **2009**, *74*, 6936−6943. (c) Robiette, R.; Aggarwal, V.

DOI: 10.1021/acs.joc.6b00559
J. Org. Chem. 2016, 81, 5303−5313

K.; Harvey, J. N. *J. Am. Chem. Soc.* **2007**, *129*, 15513−15525. (d) Dong, L.; Qin, S.; Su, Z.; Yang, H.; Hu, C. *Org. Biomol. Chem.* **2010**, *8*, 3985−3991.
(28) (a) Wang, X. F.; Peng, L.; An, J.; Li, C.; Yang, Q. Q.; Lu, L. Q.; Gu, F. L.; Xiao, W. J. *Chem. - Eur. J.* **2011**, *17*, 6484−6491. (b) Ding, L. N.; Fang, W. H. *J. Org. Chem.* **2010**, *75*, 1630−1636. (c) Li, W.; Huang, D.; Lv, Y. *Org. Biomol. Chem.* **2013**, *11*, 7497−7506.
(29) (a) Kozuch, S.; Shaik, S. *J. Am. Chem. Soc.* **2006**, *128*, 3355−3365. (b) Kozuch, S.; Shaik, S. *J. Phys. Chem. A* **2008**, *112*, 6032−6041. (c) Uhe, A.; Kozuch, S.; Shaik, S. *J. Comput. Chem.* **2011**, *32*, 978−985. (d) Kozuch, S.; Shaik, S. *Acc. Chem. Res.* **2011**, *44*, 101−110. (e) Kozuch, S.; Martin, J. M. L. *ACS Catal.* **2012**, *2*, 2787−2794. (f) Kozuch, S. *ACS Catal.* **2015**, *5*, 5242−5255.
(30) (a) Eyring, H. *J. Chem. Phys.* **1935**, *3*, 107−115. (b) Wigner, E. *J. Chem. Phys.* **1937**, *5*, 720−723.
(31) (a) Domingo, L. R.; Sáez, J. A. *Org. Biomol. Chem.* **2009**, *7*, 3576−3583. (b) Domingo, L. R.; Chamorro, E.; Pérez, P. *J. Org. Chem.* **2008**, *73*, 4615−4624. (c) Parr, R. G.; von Szentpály, L.; Liu, S. *J. Am. Chem. Soc.* **1999**, *121*, 1922−1924. (d) Domingo, L. R.; Aurell, M. J.; Pérez, P.; Contreras, R. *Tetrahedron* **2002**, *58*, 4417−4423. (e) Parr, R. G.; Pearson, R. G. *J. Am. Chem. Soc.* **1983**, *105*, 7512−7516. (f) Parr, R. G.; Yang, W. *Density Functional Theory of Atoms and Molecules*; Oxford University Press: New York, 1989.
(32) The global electrophilicity index ω (refs 31c and 31d), which measures the stabilization energy when the system acquires an additional electronic charge ΔN from the environment, is given in terms of the electronic chemical potential μ and chemical hardness η by the following simple expression:[31e] ω (eV) = $(\mu^2/2\eta)$. Both quantities can be calculated in terms of the HOMO and LUMO electron energies, ε_H and ε_L, as $\mu \approx (\varepsilon_H + \varepsilon_L)/2$ and $\eta \approx (\varepsilon_L - \varepsilon_H)$, respectively.[31f] The nucleophilicity index N(ref 31b), based on the HOMO energies obtained within the Kohn−Sham scheme, is defined as $N = E_{HOMO(Nu)} - E_{HOMO(TCE)}$.[31b] The nucleophilicity is taken relative to tetracyanoethylene (TCE) as a reference, because it has the lowest HOMO energy in a large series of molecules already investigated in the context of polar cycloadditions.
(33) Jaramillo, P.; Domingo, L. R.; Chamorro, E.; Pérez, P. *J. Mol. Struct.: THEOCHEM* **2008**, *865*, 68−72.
(34) (a) Ajitha, M. J.; Suresh, C. H. *J. Org. Chem.* **2012**, *77*, 1087−1094. (b) Gusev, D. G. *Organometallics* **2009**, *28*, 6458−6461.

DOI: 10.1021/acs.joc.6b00559
J. Org. Chem. 2016, 81, 5303−5313